Molecular Cell, Volume *82*

Supplemental information

The Mettl3 epitranscriptomic writer amplifies p53 stress responses

Nitin Raj, Mengxiong Wang, Jose A. Seoane, Richard L. Zhao, Alyssa M. Kaiser, Nancie A. Moonie, Janos Demeter, Anthony M. Boutelle, Craig H. Kerr, Abigail S. Mulligan, Clare Moffatt, Shelya X. Zeng, Hua Lu, Maria Barna, Christina Curtis, Howard Y. Chang, Peter K. Jackson, and Laura D. Attardi

Supplemental Figure 1

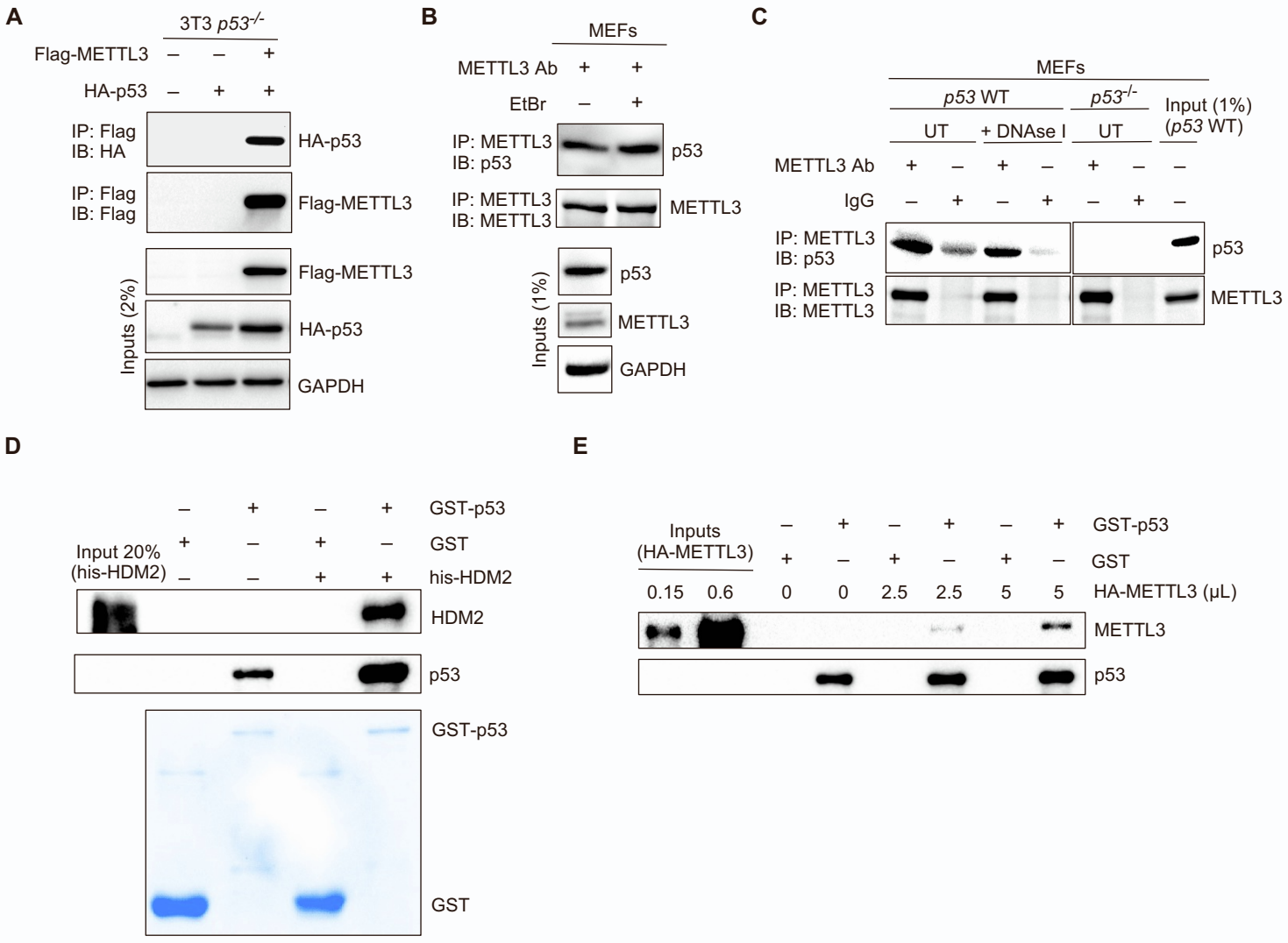

Supplemental Figure 1. p53 directly interacts with METTL3 independent of DNA, Related to Figure 1. (A) Flp-In-3T3 *p53*$^{-/-}$ cells were co-transfected with plasmids expressing Flag-METTL3 and HA-p53, and Flag-METTL3 was immunoprecipitated with anti-Flag M2 magnetic beads and detected by immunoblotting with the indicated antibodies (*n*=2). (B) CoIP and immunoblot assay to test the nucleic acid dependence of interaction between endogenous p53 and METTL3 in *E1A;HRas*^{G12V}-expressing MEFs. Lysates were pre-treated with ethidium bromide (EtBr) at 10 µg/ml prior to immunoprecipitations (*n*=2). (C) CoIP and immunoblot assay to test DNA-dependence of interaction between endogenous p53 and METTL3 in lysates from MEFs pre-treated with DNaseI (40 U/ml) to degrade DNA. IgG serves as negative control antibody. IPs in p53$^{-/-}$ cells demonstrate the specificity of the p53 antibody (*n*=2). Representative immunoblots are shown in all panels. (D) GST pull-down assays with GST and GST-tagged p53 after incubation with purified his-tagged HDM2. (Top) Binding of his-tagged HDM2 was detected by immunoblot analysis with antibodies against HDM2. (Bottom) Coomassie stained gel shows GST and GST-p53 proteins. (E) GST pull-down assays with GST and GST-tagged p53 after incubation with *in vitro* translated HA-METTL3. Binding of HA-METTL3 was detected by immunoblot analysis with antibodies against METTL3.

Supplemental Figure 2

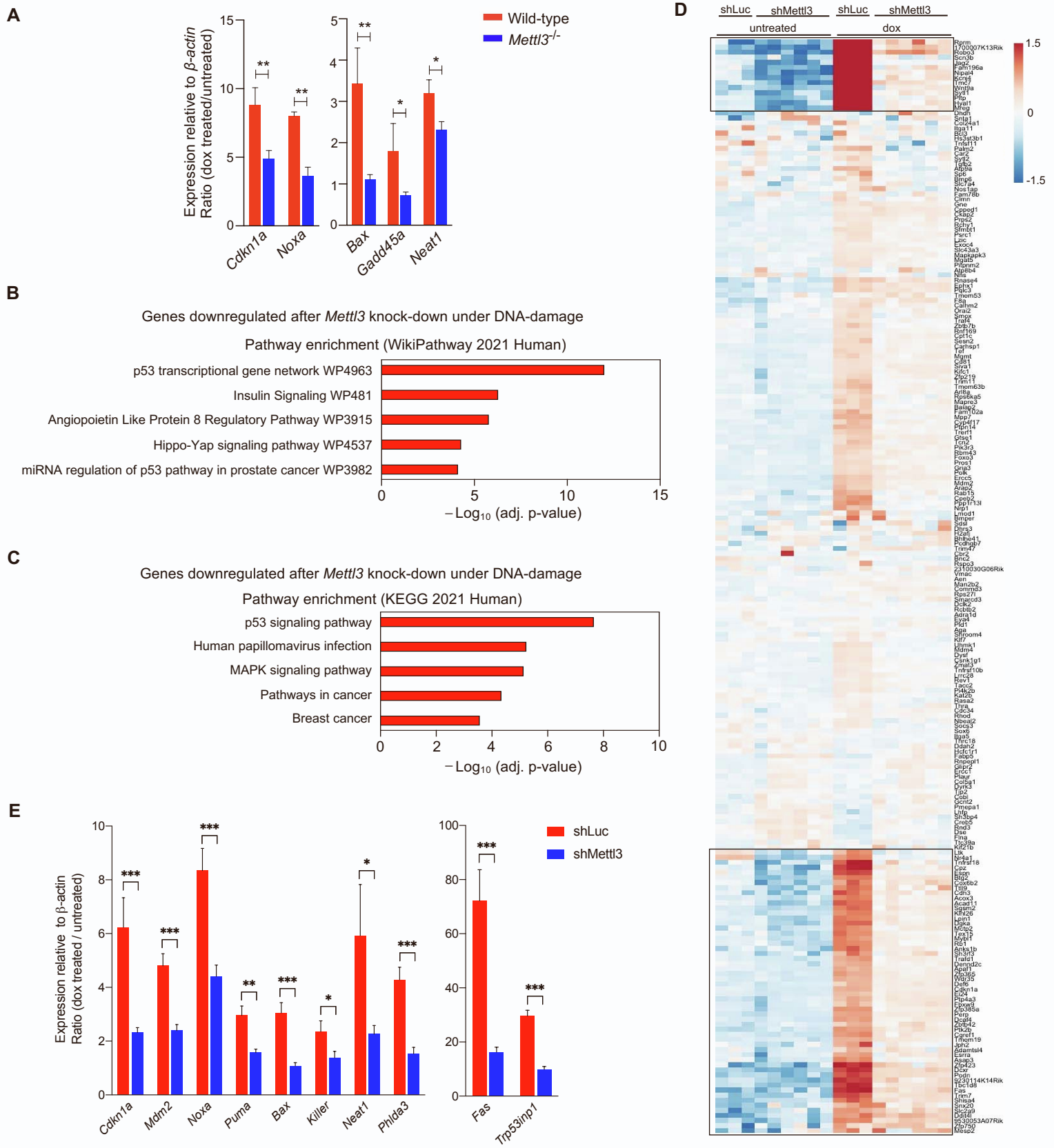

Supplemental Figure 2. *Mettl3* deficiency impairs p53 target gene induction in response to DNA damage, Related to Figure 2. (A) Induction of p53 target genes after 6 hours dox (0.2 μg/mL) in *Mettl3*$^{-/-}$ ES cells relative to wild-type cells, normalized to *β-Actin*. *Mettl3*$^{-/-}$ depicts mean of two different *Mettl3* null cell lines. Data are mean ± s.e.m. of at least three biological replicates each with three technical replicates. *P* values were determined by the unpaired two-tailed Student's t-test. **P*<0.05, ***P*<0.01. (B) The top five expression signatures enriched in genes downregulated in dox-treated *E1A;HRas*^{G12V} shMettl3-2 MEFs relative to dox-treated *E1A;HRas*^{G12V} shLuc MEFs, as identified by Enrichr analysis of WikiPathway 2021 Human (B) and KEGG 2021 Human (C) data sets. (D) Heat map showing expression patterns of all previously characterized p53-bound and p53-regulated target genes in *E1A;HRas*^{G12V} (Valente et al., 2020) in RNA-seq analysis of untreated or dox-treated shLuc and shMettl3 *E1A;HRas*^{G12V} MEFs. Genes with the highest magnitude changes, within the black boxes, were selected to generate the heat map shown in figure 2G. (E) qRT-PCR analysis of expression of p53 target genes after 6 hours dox (0.2 μg/mL) in shLuc and shMettl3 shRNA-expressing *E1A;HRas*^{G12V} MEFs, normalized to *β-Actin*. shMettl3 depicts mean of cell lines expressing either of two different shRNAs targeting *Mettl3*. Representative data are shown from two biological replicates each with three technical replicates and two different MEF lines per genotype were used. Data are mean of fold induction (Ratio of dox treated / untreated) ± s.e.m. *P* values were determined by the unpaired two-tailed Student's t-test. **P*<0.05, ***P*<0.01, ****P*<0.001.

Supplemental Figure 3

A

shLuc (dox)

Rank	Motif	*P*-value	% of Targets
1		1E-916	71.6%
2		1E-287	29.89%
3		1E-280	1.59%
4		1E-278	1.66%
5		1E-263	2.08%

shMettl3-2 (dox)

Rank	Motif	*P*-value	% of Targets
1		1E-1110	65.75%
2		1E-320	1.00%
3		1E-279	38.57%
4		1E-223	28.63%
5		1E-189	1.25%

B

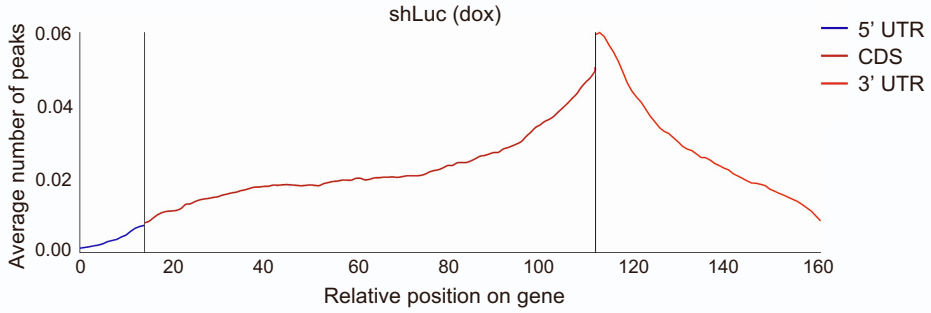

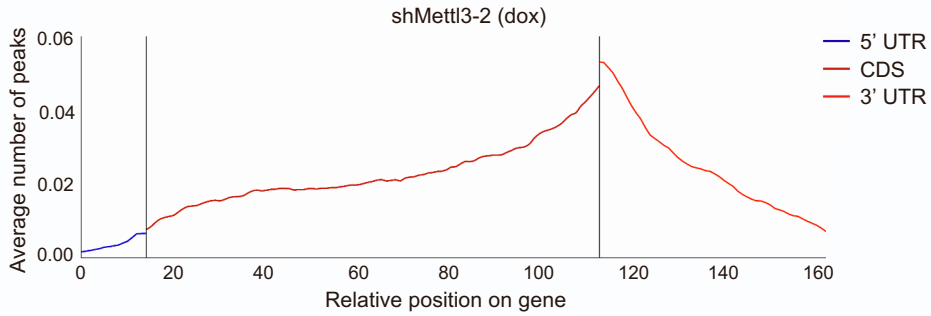

C

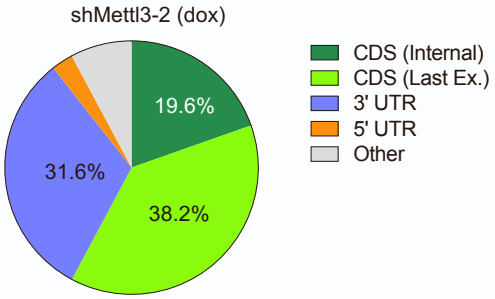

Supplemental Figure 3. Motif identification and distribution of m^{6}A-peaks in doxorubicin treated *E1A;HRas^{G12V}*-expressing MEFs, Related to Figure 4. (A) Top five sequence motifs enriched in m^{6}A-modified mRNAs in dox treated MEFs expressing shLuc control or shMettl3 RNAs. (B) Metagene plot of mRNAs displaying m^{6}A modification in dox treated MEFs expressing shLuc control or shMettl3 RNAs. Plot depicts average number of peaks mapped to certain genomic regions. The number of peaks is calculated for each region of every gene, the lengths of the regions are then normalized, and the average number of peaks for a set number of positions along the regions are calculated. (C) Pie chart of the frequency distribution of m^{6}A peaks that map to the listed mRNA features in dox treated MEFs expressing shMettl3 RNA. m^{6}A-IP reads were normalized to the total number of reads covering the m^{6}A residue in the input.

Supplemental Figure 4

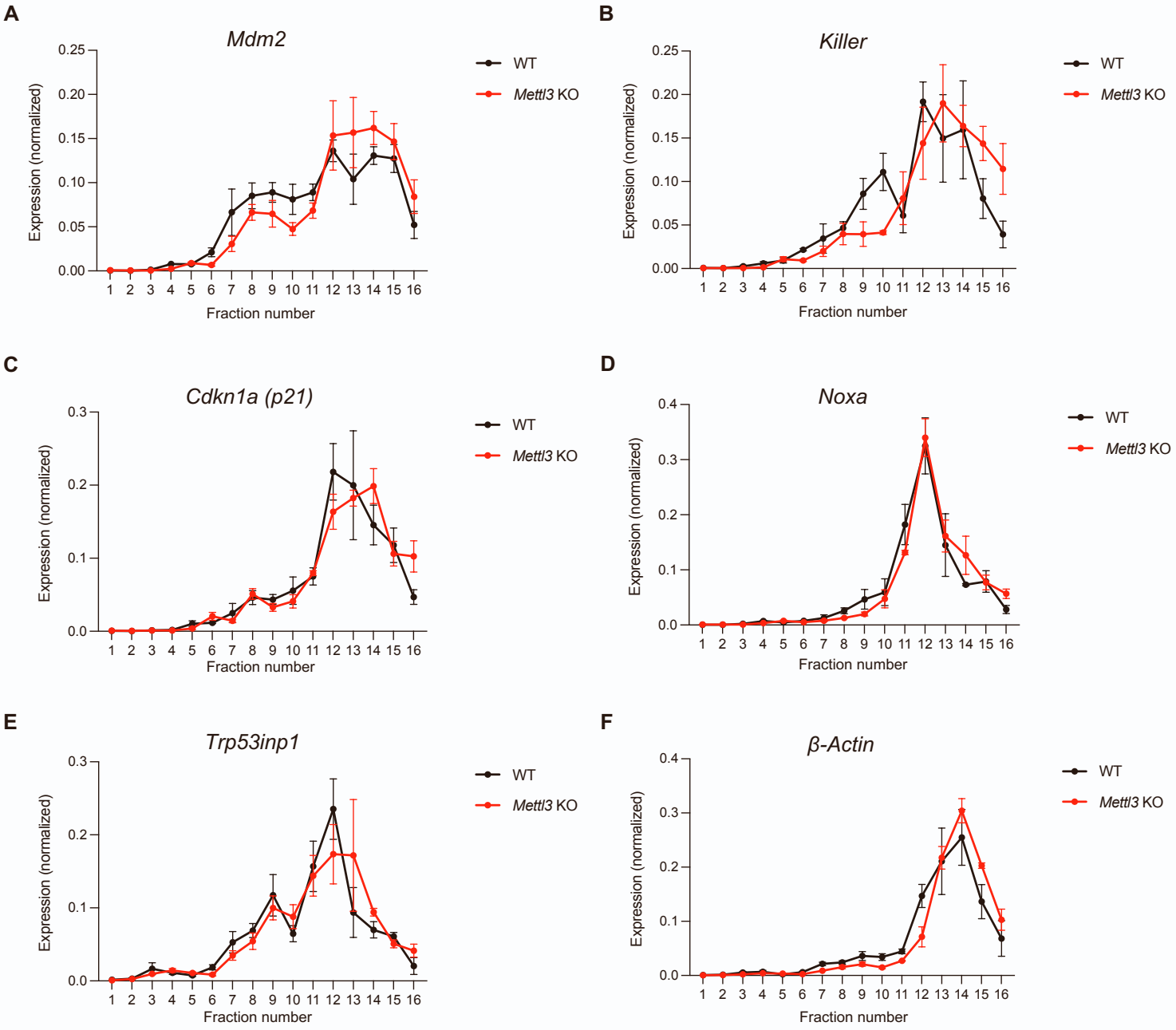

Supplemental Figure 4. Sucrose gradient polysome fractionation of mouse ES cells followed by RT-qPCR analysis of selected m^{6}A-modified and unmodified p53 target genes, Related to Figure 4. RT-qPCR analysis of m^{6}A-modified mRNAs, *Mdm2* (A) & *Killer* (B), unmodified mRNAs, *Cdkn1a, Noxa, Trp53inp1* (C-E) and control housekeeping gene *β-Actin* (F) from 15-45% sucrose density gradients from WT (black line) or *Mettl3* KO (red line) mouse ES cells treated with 8 hours dox (0.2 μg/mL). RT-qPCR Ct values were normalized to spike-in *in vitro* transcribed Renilla luciferase RNA to each fraction and then to the sum total of all fractions. Data are mean of 3 biological replicates ± s.e.m.

Supplemental Figure 5

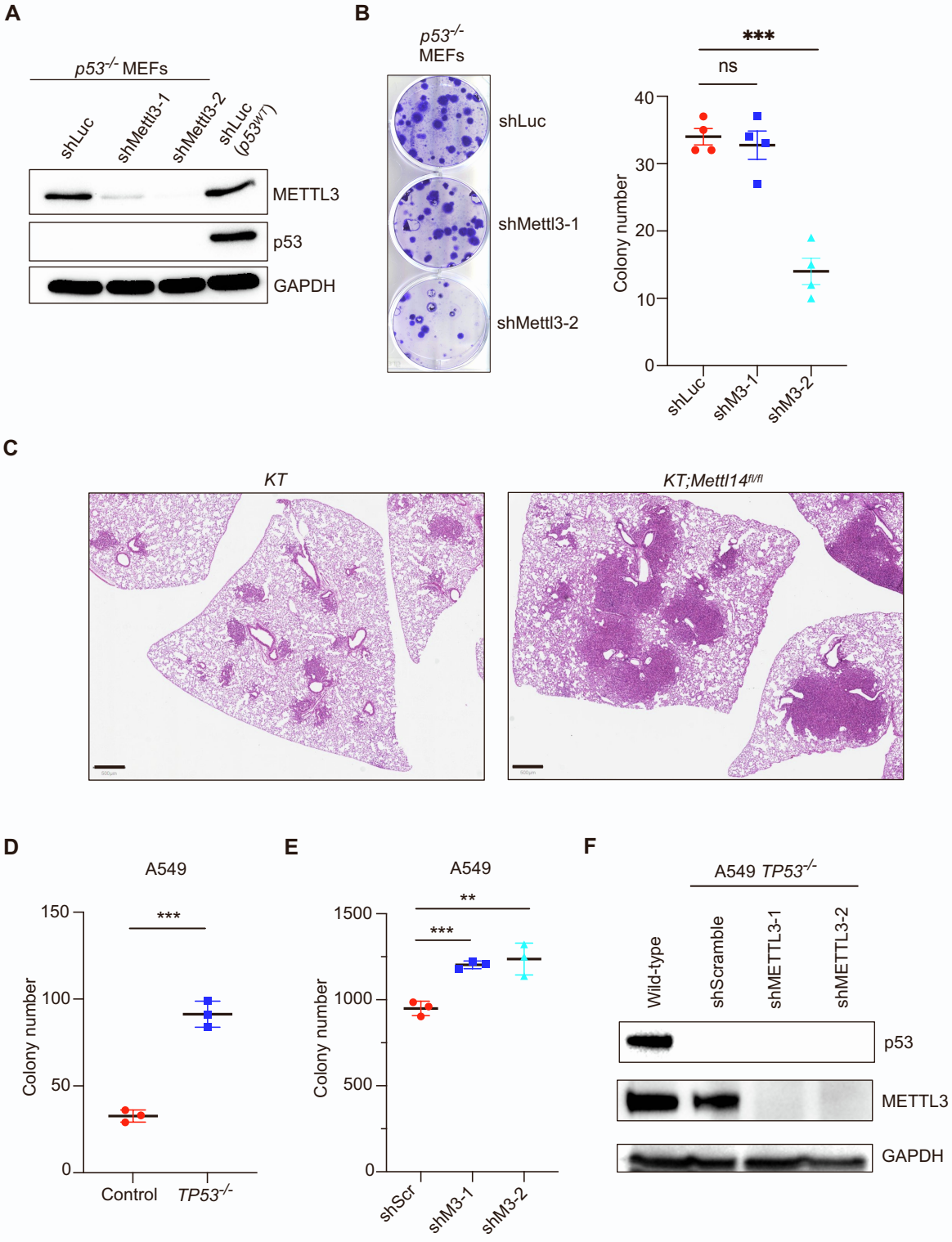

Supplemental Figure 5. METTL3 supports p53 in colony formation in MEFs and A549 cells and METTL14 has tumor suppressor activity in mouse lung adenocarcinoma, Related to Figures 6 and 7. (A) Immunoblotting for p53 and METTL3 proteins in *E1A;HRas*^{G12V}-expressing *p53*$^{-/-}$ MEFs transduced with either shLuc or shMettl3 RNAs (*n*=2). (B) Low density plating assay to assess clonogenic potential of *E1A;HRas*^{G12V}-expressing *p53*$^{-/-}$ MEFs transduced with lentiviruses expressing either shLuc or shMettl3 RNAs. (Left) Representative crystal-violet stained colonies are shown. (Right) Average colony number (n=2 with triplicate samples). (C) Representative images of H&E staining of lung tissue section from control *KT* (left panel) and *KT;Mettl14*$^{fl/fl}$ (right panel) mice infected with Ad-CMV-Cre adenovirus. Scale bar = 500 μM. *P* values were determined by the unpaired two-tailed Student's *t*-test. ***P<0.001, ns=not significant. (D) Clonogenic potential of *TP53* WT and *TP53*$^{-/-}$ A549 cell lines assayed using low density plating assay. Dots represent average colony numbers from triplicate samples (n=1). (E) Anchorage-independent growth of A549 cells upon the introduction of control shScramble (shScr) or two different shRNAs against *METTL3* (shM3-1 and shM3-2). Dots represent average colony numbers for triplicate samples from two independent experiments. (F) Immunoblotting for endogenous p53 and Flag-METTL3 proteins in A549 *TP53*$^{-/-}$ cells. GAPDH serves as loading control. *P* values were determined by the unpaired two-tailed Student's t-test. **P<0.01, ***P<0.001.

Supplemental Figure 6

A

Pan-cancer ME

gene	*P* value	*Q* value
MTC	4.99E-14	5.48E-13
ZC3H13	1.35E-11	6.93E-11
RBM15	3.57E-07	1.35E-06
MTC (core)	2.19E-06	7.4E-06
RBM15B	9.79E-06	2.72E-05
VIRMA	2.26E-05	5.83E-05
METTL14	0.000145	0.000326
WTAP	0.000631	0.001361
METTL3	0.001886	0.003998
CBLL1	0.00275	0.00535

B

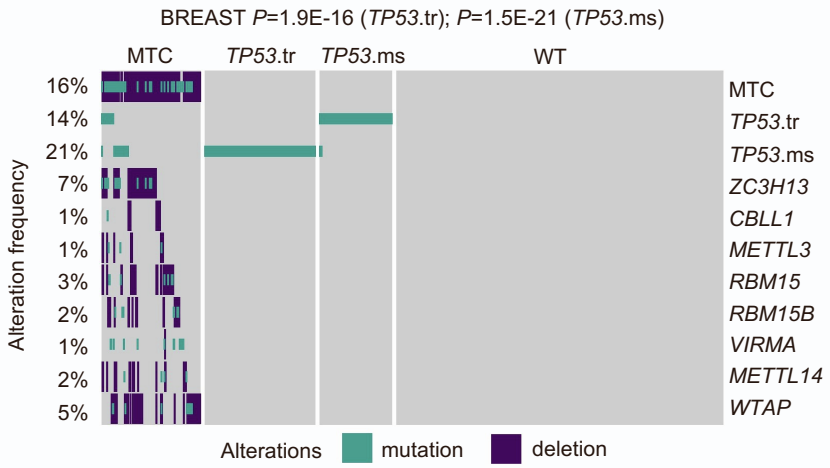

C

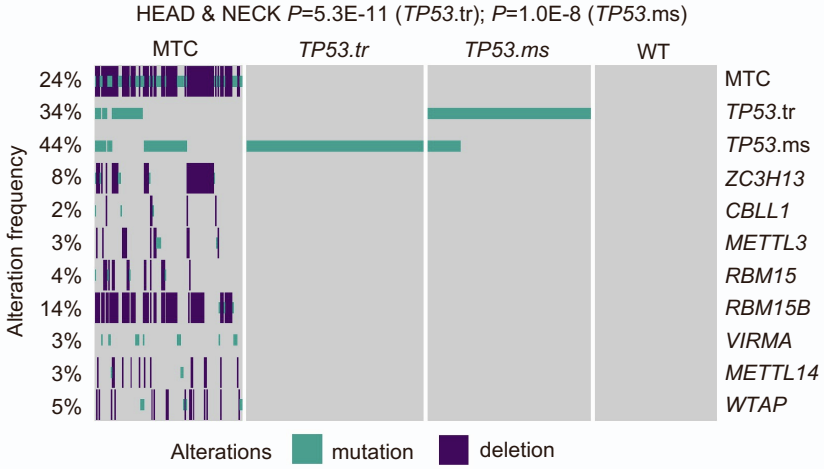

D

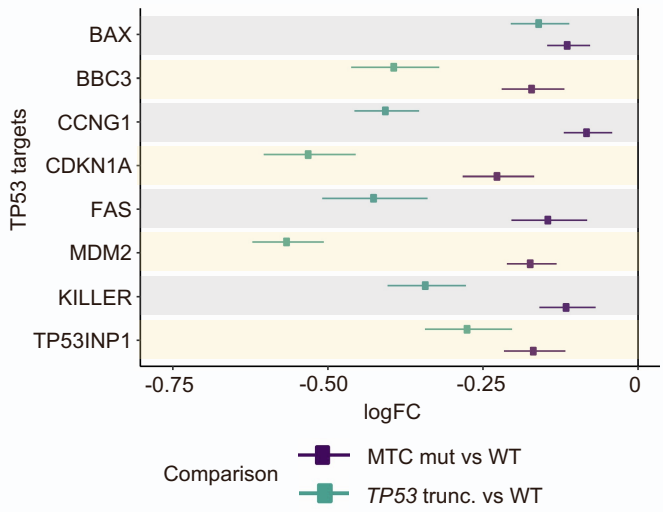

E

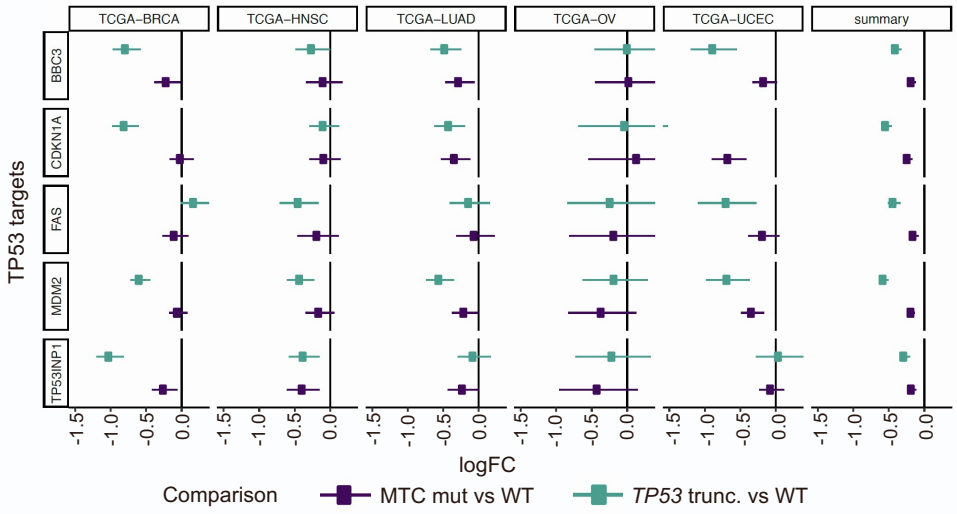

Supplemental Figure 6. Mutual Exclusivity between *TP53* and *METTL3* methyltransferase complex and differential expression (DE) analysis of *TP53* target genes in human cancers, Related to Figure 7. (A) Pan-cancer mutual exclusivity analysis using DISCOVER algorithm. (B & C) Oncoplots showing alteration frequencies of METTL3-METTL14 methyltransferase complex components in human breast and head & neck cancers. In A-C, MTC refers to any of the complex members while MTC (core) refers to METTL3, METTL14 and WTAP. TP53.tr refers to truncation mutations, while TP53.ms refers to missense mutations in *TP53*. *P* and *Q* values show significance of DISCOVER test unadjusted and adjusted for multiple testing. (D) Dots represent log fold change expression of select p53 targets in METTL3 complex (MTC) mutant vs wild-type and *TP53* truncation mutant vs wild-type tumors. Summary represents DE in 33 TCGA cancer types. (E) Dots represent log fold change expression of select p53 targets in METTL3 complex (MTC) mutant vs wild-type and *TP53* truncation mutant vs wild-type tumors, in human lung adenocarcinoma (LUAD), breast cancer (BRCA), ovarian cancer (OV), uterine corpus endometrial carcinoma (UCEC) and head and neck squamous cell carcinoma (HNSCC). Summary represents DE in the five cancer types shown on the left. In (D) and (E), MTC refers to any of the METTL3 complex members, while *TP53* trunc. refers to truncation mutations in *TP53*.

Supplemental Figure 7

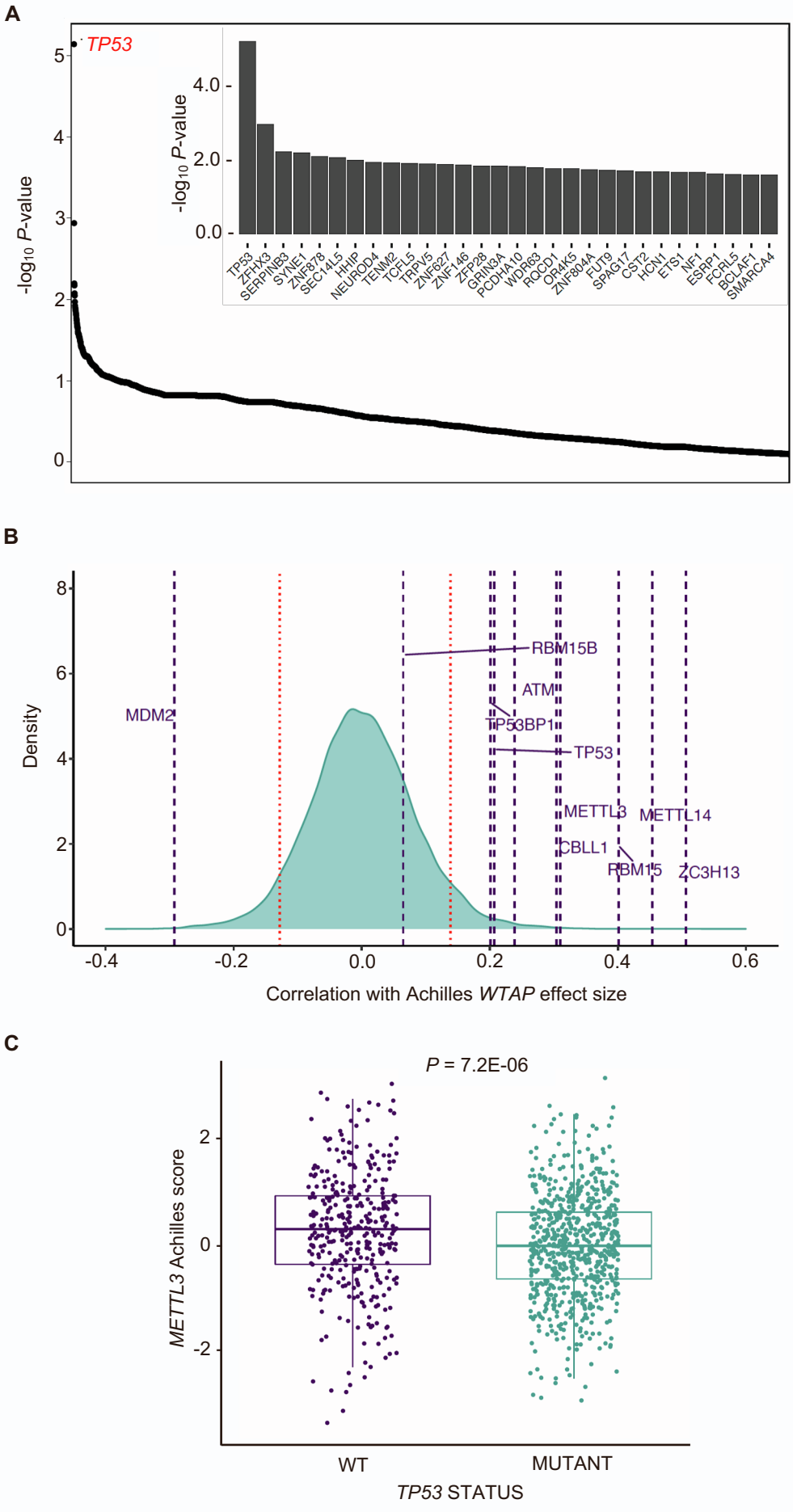

Supplemental Figure 7. METTL3 and TP53 operate in the same pathway, Related to Figure 7. (A) METTL3 Achilles score association with all genes with any mutation across the DepMap ($-\log_{10}$ P-value). P values were calculated by a Wilcoxon signed-rank test. (B) Density distribution of Pearson correlations between WTAP Achilles scores. Horizontal lines represent genes of interest including MTC components, TP53, and regulators of p53 pathway. Red bars represent the 5th and 95th quantiles of the distribution. (C) Achilles scores for *METTL3* in *TP53* WT and *TP53* mutant cell lines.

Supplemental Table 1

p53 BP	Mean NSAF	p53 BP	Mean NSAF	p53 BP	Mean NSAF	p53 BP	Mean NSAF
4921504E06RIK	0.000223	EIF4G1	0.004144	MYO5A	0.000932	RRBP1	0.000862
ABCF2	0.001081	ELAVL1	0.000662	NAGLU	0.000893	RREB1	0.000256
ABRAXAS2	0.001232	EPB41L3	0.002060	NCL	0.004723	RTCB	0.002644
ACACA	0.001319	EPRS	0.000795	NDC1	0.001240	RUVBL1	0.001822
ACADSB	0.000340	FARP1	0.000863	NEDD4	0.000764	SEPT11	0.000769
ACTA2	0.000819	FHOD1	0.001053	NSUN7	0.000521	SEPT9	0.000352
ACTBL2	0.000240	FLNC	0.001240	OFD1	0.000272	SERBP1	0.001685
ACTN1	0.000684	FLT4	0.000592	OPLAH	0.000488	SF3B1	0.001116
ACTN4	0.000075	FN1	0.001540	PABPC1	0.002589	SF3B3	0.001284
ACTR1B	0.001354	FUS	0.001279	PAWR	0.002055	SFPQ	0.001998
ADGRV1	0.000356	G3BP1	0.002527	PCDHGC4	0.000224	SLC25A12	0.001768
ADRM1	0.000745	GABBR2	0.014335	PDE4D	0.000660	SLC25A4	0.000783
AHNAK	0.006850	GAPDH	0.003468	PDZD8	0.000204	SMARCE1	0.000374
AHNAK2	0.000985	GEMIN5	0.000204	PFKL	0.000360	SMC2	0.000696
AIMP1	0.000482	GJC2	0.000669	PFKM	0.000966	SMC3	0.000391
ASPH	0.000331	GLMN	0.001037	PHC2	0.001414	SMG5	0.003057
ATAD3A	0.006702	GM10334	0.008535	PI4KA	0.000425	SMG7	0.003877
ATP5A1	0.001387	GM5414	0.000076	PITRM1	0.000753	SNRNP200	0.001320
C2CD2L	0.000229	GMPS	0.000909	PIWIL2	0.000509	SNX21	0.000494
CALD1	0.002456	GSTM5	0.000372	PKM	0.000426	SNX25	0.000742
CAPRIN1	0.000847	HADHA	0.001102	PML	0.000501	SOAT1	0.000649
CAVIN2	0.001352	HDLBP	0.000352	PPP1R12A	0.001376	SP3	0.000272
CCDC39	0.000340	HELLS	0.000560	PPP1R18	0.000696	SPECC1	0.001036
CCT2	0.002940	HNRNPA1	0.002042	PRPF19	0.001580	SPEN	0.000447
CCT3	0.001675	HNRNPAB	0.001656	PRPF3	0.000759	SPTAN1	0.000465
CCT4	0.001847	HNRNPD	0.001566	PRPF6	0.000760	SPTBN1	0.000635
CCT5	0.002269	HNRNPH1	0.002860	PSMA1	0.002276	SRSF2	0.002069
CCT6A	0.002208	HNRNPK	0.001424	PSMA2	0.001318	SWT1	0.000340
CCT7	0.002086	HNRNPL	0.002632	PSMA3	0.001836	SYNE1	0.000102
CCT8	0.003049	HNRNPM	0.001819	PSMA4	0.000908	SYTL4	0.004656
CDK12	0.000493	HNRNPU	0.004875	PSMA5	0.001291	TAF15	0.001246
CNOT1	0.000152	HNRNPUL2	0.002646	PSMA6	0.001689	TCP1	0.003513
COL1A1	0.000152	HPS3	0.000038	PSMA7	0.001710	THBS1	0.000458
COPB1	0.000713	HSPA4	0.000351	PSMB1	0.001889	THOC2	0.001849
COPB2	0.000696	HSPH1	0.001918	PSMB2	0.001188	TLN1	0.000722
CTNNA1	0.000849	HYDIN	0.002615	PSMB3	0.000922	TMPO	0.001927
CUL1	0.002177	IARS	0.000653	PSMB4	0.001033	TNRC6B	0.000204
CUL5	0.001355	IL1RAPL1	0.001266	PSMB5	0.001928	TPM4	0.000418
CYLC1	0.001019	IQGAP3	0.001172	PSMB6	0.000994	TRIM24	0.002180
DAPK1	0.000102	JUP	0.003969	PSMB7	0.001134	TRIM28	0.003184
DCTN2	0.005310	KIF20B	0.000836	PSMC1	0.004313	TRRAP	0.005174
DCTN4	0.001812	KIF26A	0.000102	PSMC2	0.005191	TTN	0.000709
DDX1	0.001865	KIF4	0.000129	PSMC3	0.004956	TUFM	0.000389
DDX17	0.001622	KIF5B	0.000608	PSMC4	0.003626	TXLNG	0.000244
DDX3X	0.004738	LARP1	0.000558	PSMC5	0.005480	UBAP2L	0.003702
DDX42	0.000408	LETM1	0.000764	PSMD1	0.006147	UBC	0.013240
DLAT	0.000643	LOC105242472	0.000436	PSMD12	0.003606	UBR2	0.001401
DOCK9	0.000114	LOX	0.002025	PSMD13	0.002487	UBR4	0.000793
DSG1B	0.000632	LRPPRC	0.001426	PSMD14	0.002128	UBTF	0.001960
DUSP8	0.000246	MAP1A	0.000408	PSMD2	0.007069	USP7	0.001859
DVL2	0.000645	MAP1B	0.000669	PSMD3	0.003821	UTRN	0.001314
DYNC1H1	0.001856	MAP4	0.000332	PSMD4	0.002189	VARS	0.000660
EEF1A2	0.000102	MAPK3	0.000076	PSMD6	0.002300	VCPIP1	0.001030
EEF1D	0.001147	MARCKS	0.000986	PSMD7	0.000852	VPS35	0.000160
EEF1G	0.000379	MAST4	0.001698	PSMD8	0.000811	WDR5	0.000459
EFCAB12	0.000187	MCM3	0.000779	RAD23A	0.000595	ZBTB25	0.000176
EFEMP1	0.000986	MCM5	0.001131	RAD50	0.001240	ZFP819	0.000204
EFTUD2	0.000775	MCM9	0.000288	RAI14	0.001495		
EIF2S1	0.000271	MDM2	0.015265	RALGAPA2	0.009169		
EIF3B	0.002838	MDM4	0.001648	RANGAP1	0.000624		
EIF3F	0.001811	METTL3	0.000344	RBM14	0.002547		
EIF3H	0.002058	MFGE8	0.002276	RBMXL1	0.003311		
EIF3I	0.001239	MOGS	0.000625	RHOX5	0.001065		
EIF3L	0.002683	MRVI1	0.000306	RNH1	0.009212		
EIF4B	0.001059	MYH9	0.001024	RPAP1	0.000673		

Supplemental Table 1. List of p53 binding proteins (BP) identified in p53-LAP AP-MS under DNA-damage treatment, Related to Figure 1. Numbers indicate the mean NSAF values from three replicate experiments.

Supplemental Table 4

qRT-PCR primers:

Gene	Forward Primer (5'-3')	Reverse Primer (5'-3')
Cdkn1a	CACAGCTCAGTGGACTGGAA	ACCCTAGACCCACAATGCAG
Noxa	GCAGAGCTACCACCTGAGTTC	CTTTTGCGACTTCCCAGGCA
Bax	TGAAGACAGGGGCCTTTTTG	AATTCGCCGGAGACACTCG
Gadd45a	CTCGGCTGCAGAGCAGAAGA	GGCACAGTACCACGTTATCG
Neat1	CCTGGGGATGAGGCCTGGTCT	GGCCAGAGCTGTCCGCCC
Mdm2	CTGTGTCTACCGAGGGTGCT	CGCTCCAACGGACTTTAACA
Puma	GCGGCGGAGACAAGAAGA	AGTCCCATGAAGAGATTGTACATGAC
Killer	AACACGGAACCTGGCAAGA	TTTCCGTTTACCGGAACCA
Phlda3	TTCGCCCGCATCAAAGCCGT	AGGGGGCAGCGGAAGTCG AT
Fas	CTGCGATGAAGAGCATGGTT	GCGCAGCGAACACAGTGTT
Trp53inp1	CTTCTTCCAGCCAAGAACCA	CTGAGAAACCAGGGCAGGTA
β-Actin	TCCTAGCACCATGAAGATCAAGATC	CTGCTTGCTGATCCACATCTG

ChIP-qPCR primers:

Gene	Forward Primer (5'-3')	Reverse Primer (5'-3')
Cdkn1a	GAGACCAGCAGCAAAATCG	CAGCCCCACCTCTTCAATTC
Noxa	AAGCAATTTGGGGGTTGAG	GAGCGAAGTGGAGCAGGTC
Neat1	GAATCTGCAAGCAAGGCCCGG	GAGCAAGCCAGCACTTGCCACATA
Mdm2	CTTCCTGTGGGGCTGGTC	CGGGGCAGCGTTTAAATAAC
Killer	GGGTTTCGGATGAGCTGACA	CAAGCAGCAACGCAAAGCTA
Trp53inp1	CTCACGTAAGTGCGGGCTAC	GGAGAGAGTCCGGCATGAAA

Supplemental Table 4. Primer sequences, Related to STAR Methods.